

LARGE EDDY SIMULATION OF THE FLOW AROUND A WIND TURBINE BLADE

Andrei Shishkin* and Claus Wagner†

German Aerospace Center, Bunsenstr. 10, D-37073, Göttingen, Germany

*e-mail: Andrei.Shishkin@dlr.de

† e-mail: Claus.Wagner@dlr.de

Key words: Large eddy simulation, wind turbine blade, flow separation, complex geometry, mesh generation, hp-refinement

Abstract. *Large Eddy Simulations (LES) of incompressible turbulent flow around a wind turbine blade at a chord Reynolds number of 5×10^3 are performed using a high-order spectral/hp element method ($S_{hp}EM$). The method and the early results of the simulations are presented. Some requirements with respect to mesh generation for the $S_{hp}EM$ concerning h- and p-refinement and the estimation of the mesh quality are discussed.*

1 INTRODUCTION

During the last years wind turbine aerodynamics is the subject of an increasing interest and was therefore addressed in a number of experimental and numerical research projects. One of the most difficult problems is the computation of extreme loads caused by wind gusts. Some of the traditional approaches, like Reynolds-averaged Navier-Stokes (RANS) simulation, can not be successfully applied due to the unsteady nature of the problem. In this respect, the Large Eddy Simulation (LES) has proven to be useful technique to simulate the unsteady flow around airfoils.

The European LESFOIL project which ended in 2001 was an essential step forward in the practical using of LES as alternative to RANS modeling. The airfoil geometry selected for investigations was the Aerospatiale-A airfoil. The Reynolds number $Re = 2.1 \cdot 10^6$ and angle of attack $\alpha = 13.3^\circ$ were considered. The results of the project are presented in the final report ¹. In the framework of this project many problems have been investigated, in particular: numerical stability for complex geometry simulation, the role of near-wall modeling and resolution for LES, the minimal size of computational domain and grid point distribution and comparison of results obtained on structured and unstructured grids.

More recently Jovičić and Breuer² investigated the turbulent flow around the NACA-4415 airfoil at chord based Reynolds number $Re = 10^5$ and angles of attack $\alpha = 18^\circ$. They carried out well-resolved LES applying the dynamic subgrid-scale model (SGS)

by Germano³ and finite volume discretization using 23.56 million control volumes. The same geometry and equal flow parameters were considered by Eisenbach and Friedrich⁴. They performed LES using numerical method based on second-order central spatial discretization and immersed boundary technique on cartesian grid. In both cases the results are in a good agreement with experimental data obtained from measurements at DLR Göttingen⁵⁻⁷.

Kim et al.⁸ studied unsteady flow around a symmetrical NACA-0018 airfoil at Reynolds number $Re = 1.6 \cdot 10^5$ and angle of attack $\alpha = 0^\circ, 3^\circ, 6^\circ, 9^\circ$. They applied Germano's dynamic SGS model with finite volume discretization on a relatively coarse H-type structured grid.

One can note that observed literature deals mainly with low-order methods and many investigated aspects of LES have to be specified in the case of high-order methods. In this respect, LES using spectral element methods is of interest even in non-airfoil cases. Ma et al.⁹ perform Direct Numerical Simulation (DNS) and LES of turbulent flow past a circular cylinder using 2D spectral/hp element method with Fourier extension along the homogeneous direction (cylinder-axis) for a different Reynolds numbers between 500 and 5000 and with spatial resolutions ranging from $2 \cdot 10^5$ to 10^8 degrees of freedom.

The spectral/hp element approach ($S_{hp}EM$) was developed by Karniadakis and Sherwin¹⁰, T. Warburton¹¹, Karamanos^{12,13} and co-workers. This method provides high (spectral) accuracy, works on hybrid structured/unstructured meshes, admits h - and p -refinement and has its strength in dealing with complex computational domains. Some aspects of using $S_{hp}EM$ for DNS of turbulent pipe flow at low Reynolds number were studied by Shishkin and Wagner¹⁴. The authors experienced that $S_{hp}EM$ requires caution with the mesh generation and to the choice of simulation parameters with respect to the numerical stability at moderate and high Reynolds numbers and to computational costs.

The work presented in this article is a part of the ongoing research project "Innovation und neue Energietechnologien" funded by the BMWA, Germany. The partial aim of the project is the numerical simulation and the analysis of a turbulent flow around a wind turbine blade with respect to the flow separation on the blade close to stall and the effect of wind gusts on the blade. Here we present early results obtained in LES of turbulent flow around a FX-79-W151 airfoil profile at Reynolds number based on chord length cl and freestream velocity $Re_{cl} = 5 \cdot 10^3$ using $S_{hp}EM$.

2 COMPUTATIONAL DETAILS

We simulate a turbulent flow around a wind turbine blade for a Reynolds number, based on freestream velocity U_∞ , chord length cl of the blade profile and kinematic viscosity ν , of $Re = \frac{U_\infty cl}{\nu} = 5 \cdot 10^3$ and angle of attack $\alpha = 12^\circ$.

The computational domain is schematically shown in Fig. 1. The inlet boundary is placed $\approx 15cl$ upstream of the leading edge of the blade and the outlet boundary is placed $\approx 30cl$ downstream of the trailing edge. In the cross-flow direction the computational domain extends from $-15cl$ to $15cl$. The spanwise length L_z is taken equal to $\pi \cdot cl$. The

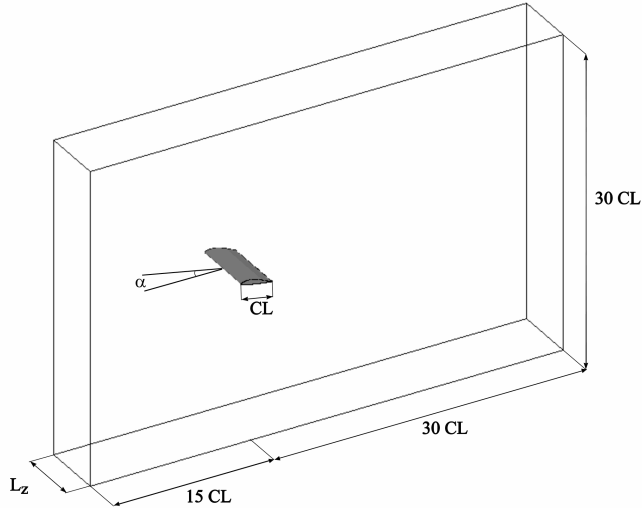


Figure 1: Schematic view of the computational domain

boundary conditions used are Neumann boundary conditions at the outflow and on the sides of domain, and periodical in spanwise direction. The initial data are obtained from the Direct Numerical Simulation (DNS) by Stoevesandt et al.¹⁵.

We use the spectral/hp element method based on the high order polynomial representation of the solution combined with the Fourier extension in homogenous spanwise direction. This method was developed by Karniadakis¹⁰, Sherwin^{10,13}, Warburton¹¹, Karamanos¹² and co-workers and implemented in *NekTar* code. A short description of the algorithm is provided in the next section.

For the LES the flow is described by the dimensionless filtered Navier-Stokes equations

$$\nabla \cdot \tilde{\mathbf{u}} = 0, \quad \frac{\partial \tilde{\mathbf{u}}}{\partial t} + (\tilde{\mathbf{u}} \cdot \nabla) \tilde{\mathbf{u}} = -\nabla \tilde{p} + \nabla \cdot [(\nu + \nu_s) (\nabla \tilde{\mathbf{u}} + (\nabla \tilde{\mathbf{u}})^T)], \quad (1)$$

where $\tilde{\mathbf{u}}$ and \tilde{p} denote the filtered velocity and pressure fields, respectively. Smagorinsky eddy-viscosity model is presented by the term $\nu_s = l_s^2 |\tilde{S}|$, where l_s is the Smagorinsky length scale, and $|\tilde{S}|$ is the magnitude of the strain rate tensor. Smagorinsky length scale l_s is depended on filter width Δ as $l_s = c_s \Delta$, where c_s is the Smagorinsky constant. In our simulations c_s is taken equal to 0.1. As proposed by Karamanos¹², the filter width Δ depends on element area A , polynomial order P and the grid spacing in the Fourier direction Δz as follows

$$\Delta = \left(A \left(\frac{\pi}{P} \right)^2 \Delta z \right)^{1/3}. \quad (2)$$

3 NUMERICAL METHOD

The time dependent spatially varying viscosity in Eq.(1) is decomposed to two components $\bar{\nu} + \nu'$, where $\bar{\nu}$ is a time independent component and ν' is a spatially and temporally varying component. So, the linear term of Eq.(1) can be rewritten as a sum of two parts

$$L^+(\tilde{\mathbf{u}}) = \nabla \cdot (\bar{\nu} \nabla \tilde{\mathbf{u}}) = \bar{\nu} \nabla^2 \tilde{\mathbf{u}} \quad (3)$$

and

$$N^+(\tilde{\mathbf{u}}) = \nabla \cdot (\bar{\nu} (\nabla \tilde{\mathbf{u}})^T) + \nabla \cdot [\nu' (\nabla \tilde{\mathbf{u}} + (\nabla \tilde{\mathbf{u}})^T)]. \quad (4)$$

With these notations Eq.(1) reads

$$\frac{\partial \tilde{\mathbf{u}}}{\partial t} + N(\tilde{\mathbf{u}}) = -\nabla \tilde{p} + L^+(\tilde{\mathbf{u}}) + N^+(\tilde{\mathbf{u}}), \quad (5)$$

where $N(\tilde{\mathbf{u}}) = (\tilde{\mathbf{u}} \cdot \nabla) \tilde{\mathbf{u}}$. The meaning of the decoupling of the linear term is to apply the high order splitting scheme for Navier-Stokes equations proposed by Karniadakis, Israeli & Orszag¹⁶ (see also Karniadakis&Sherwin¹⁰) with one modification: the term $N^+(\tilde{\mathbf{u}})$ is treated explicitly together with non-linear term $N(\tilde{\mathbf{u}})$.

This leads to the following process.

1. Integrate explicitly non-linear term.

$$\frac{\tilde{\mathbf{u}}^* - \tilde{\mathbf{u}}^n}{\Delta t} = \sum_{q=0}^{J-1} \beta_q [N(\tilde{\mathbf{u}}^{n-q}) + N^+(\tilde{\mathbf{u}}^{n-q})], \quad (6)$$

where $\tilde{\mathbf{u}}^*$ is intermediate velocity, β_q , ($q = 0, \dots, J-1$) are the coefficients of explicit Adams-Bashforth scheme of order J , and γ_q – the coefficients of implicit scheme.

2. Solve the Poisson equation for pressure p^{n+1}

$$\nabla^2 p^{n+1} = \nabla \cdot \left(\frac{\tilde{\mathbf{u}}^*}{\Delta t} \right) + \nabla \cdot \left[\sum_{q=0}^{J-1} \gamma_q L^+(\tilde{\mathbf{u}}^{n+1-q}) \right] \quad (7)$$

with the wall boundary conditions

$$\frac{\partial p^{n+1}}{\partial \mathbf{n}} = \mathbf{n} \cdot \left[\sum_{q=0}^{J-1} \beta_q (N(\tilde{\mathbf{u}}^{n-q}) + N^+(\tilde{\mathbf{u}}^{n-q})) + \sum_{q=0}^{J-1} \gamma_q L^+(\tilde{\mathbf{u}}^{n+1-q}) \right]. \quad (8)$$

The unknown velocity $\tilde{\mathbf{u}}^{n+1}$, involved in the calculations, is approximated here using Adams-Bashford scheme.

3. Solve the Helmholtz equation for velocity $\tilde{\mathbf{u}}^{n+1}$

$$\frac{\tilde{\mathbf{u}}^{n+1} - \tilde{\mathbf{u}}^*}{\Delta t} = -\nabla p^{n+1} + \sum_{q=0}^{J-1} \gamma_q L^+(\tilde{\mathbf{u}}^{n+1-q}) \quad (9)$$

The implementation of this computational scheme is based on the Fast Fourier Transformation in homogeneous direction and high-order 2D polynomial representation of components of Fourier decomposition. The time integration step (Eq.6) and the calculation of pressure boundary conditions (Eq.8) are performed in physical space. The Fourier transform is applied to solve equations (7) and (9). The Fourier components of the unknown fields are sought in the form $\tilde{\mathbf{u}}(\mathbf{x}, t) = \sum_i \hat{\mathbf{u}}_i(t) \varphi_i(\mathbf{x})$, where $\{\varphi_i(\mathbf{x})\}$ is a system of piecewise polynomial base functions (modes). Each mode $\varphi_i(\mathbf{x})$ is supported by one element (triangle or quadrilateral) of the mesh. For the quadrilateral element the system $\{\varphi_i(\mathbf{x})\}$ is based on the tensor product of the classical Jacobi polynomials. In the case of triangle the modes $\varphi_i(\mathbf{x})$ are represented by the polynomials, orthogonal over a triangle, which, in turn, are expressed in terms of classical Jacoby polynomials (for details see Karniadakis and Sherwin¹⁰).

Following the standard Galerkin approach, the Fourier-transformed equations (7) and (9) take the weak form $(K + \lambda M)\hat{\mathbf{u}} = \mathbf{f}$, where K is the homogeneous stiffness matrix and M is the mass matrix and $\hat{\mathbf{u}}$ are the unknown coefficients of 2D polynomial decomposition of Fourier components of desired solutions. These linear systems are transformed to those of lower dimension applying the Schur complement (static condensation) technique, and then they are solved directly or iteratively using preconditioned conjugate gradient method.

4 MESH GENERATION

The mesh used to perform the LES consists of 1954 triangle elements and provides $\approx 3.5 \cdot 10^6$ degrees of freedom (i.e. globally independent modes) in 64 Fourier planes. To generate a mesh we use a two-step process. We construct at first a coarse finite element mesh, which we then refine with variable order of polynomial basis.

The approach used for the first step is schematically depicted on Fig. 2. The computational domain is divided into zones corresponding to the expected computational requirements which are followed from the physical properties of the flow. The first zone is a close region around the airfoil. In view of the fine resolution needed at the wall, this zone is supposed to contain up to 50% of the mesh elements including thin element layer around the airfoil. The wake region refered in Fig. 2 as zone 2 is resolved with approximately 30% of the mesh elements and the size of element decreases as departs from the trailing edge. Further refinement within the airfoil and wake regions is provided by varying the polynomial order. The near outlet region (zone 4 on the Fig. 2) is used to dissipate vortical structures.

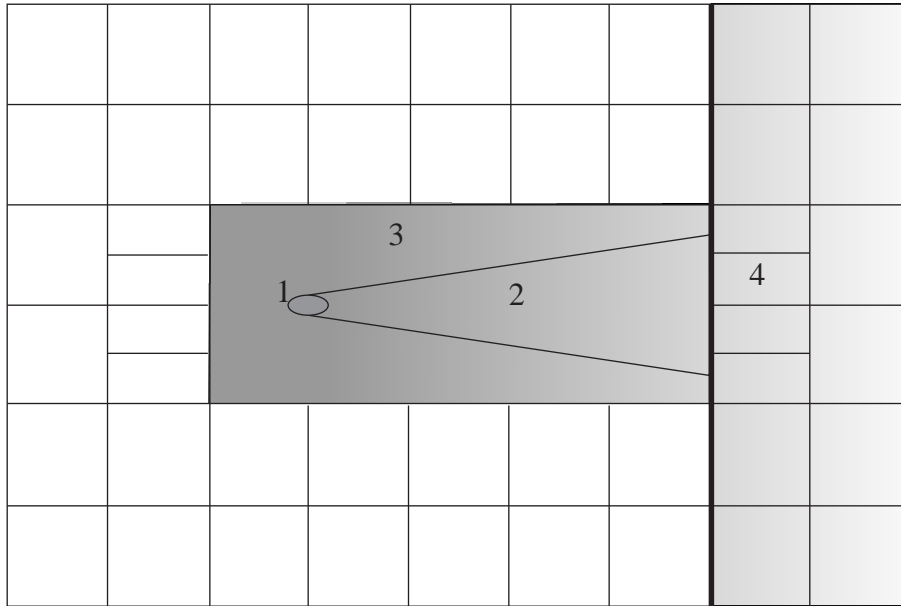


Figure 2: Scheme of the mesh construction. Distribution of the mesh elements: zone 1, near airfoil region, $\approx 50\%$; zone 2, wake region, $\approx 30\%$; zone 3 $\approx 15\%$; the rest $\approx 5\%$.

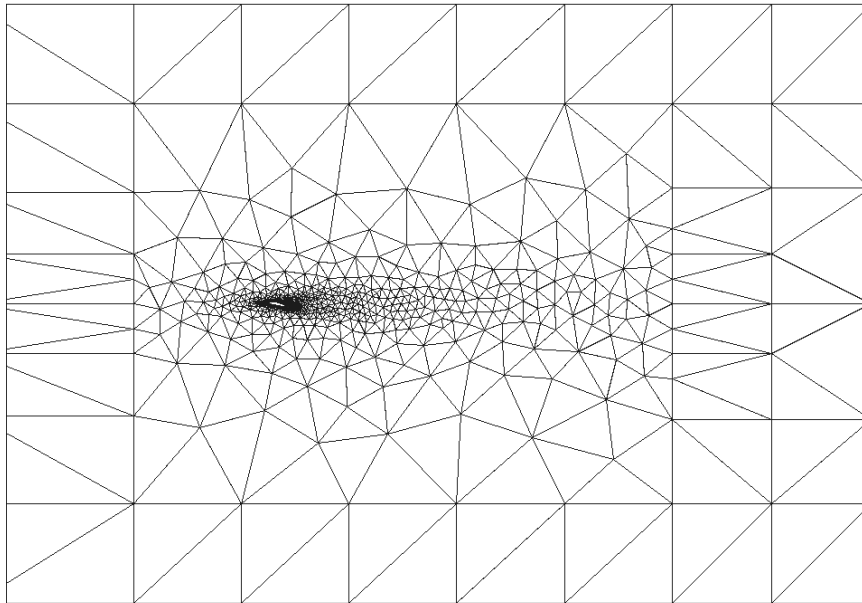


Figure 3: Triangle based 2D mesh consisting of 1954 elements.

The constructed mesh is shown in Fig. 3. Fig. 4 displays the mesh in the close region around the blade with a boundary element layer of size $3 \cdot 10^{-3}$.

The mesh quality can be estimated calculating the density of degrees of freedom for

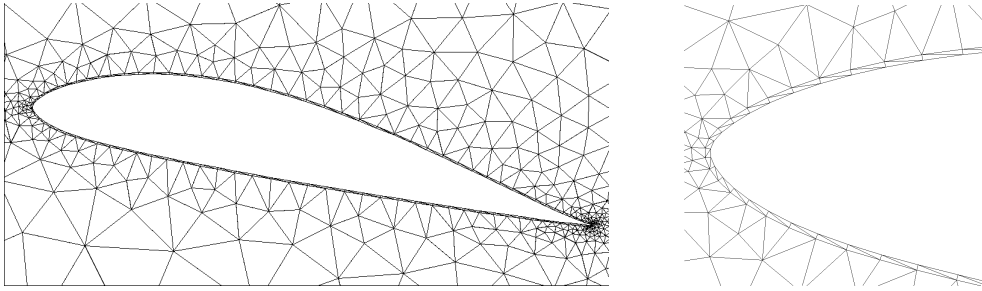


Figure 4: Left – zoom of the mesh close to the blade. Right – neighborhood of the leading edge.

each element (Shishkin and Wagner¹⁴). For the fixed polynomial order $P = 7$ the highest density equals $4.3 \cdot 10^7$ degrees of freedom per square unit and is reached in the trailing edge area. Along the airfoil profile the density is varying due to varying length of boundary elements. The lowest density in boundary element layer is of the order of 10^6 . The density decreases approaching the boundary of the computational domain. Fig. 5 shows the logarithm of density of degrees of freedom.

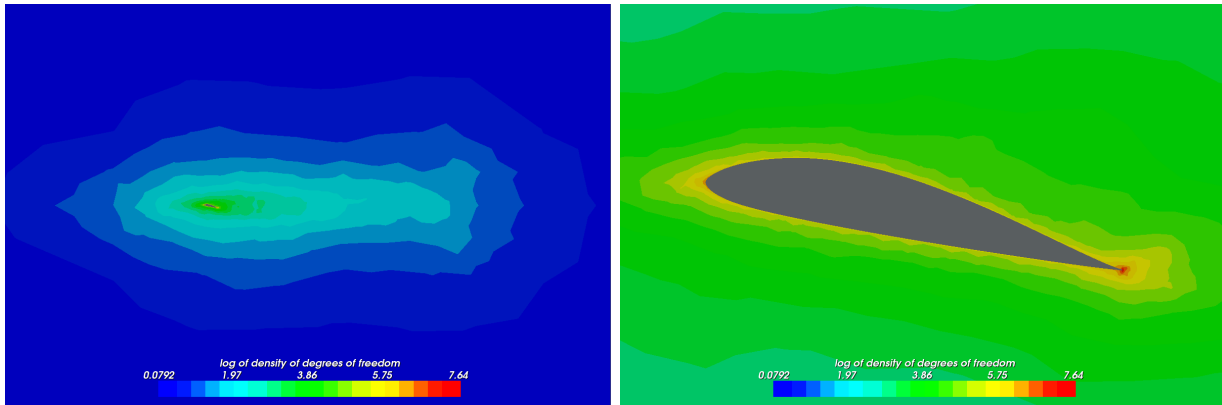


Figure 5: Density of degrees of freedom at fixed polynomial order $P = 7$. The highest density at the trailing edge equals $4.3 \cdot 10^7$ degrees of freedom per square unit.

To get a better resolution in the most important zones of the domain and to avoid an excessive resolution far away from the airfoil we apply the variable polynomial order for the mesh elements. The highest polynomial order $P = 9$ is selected in the near blade region. The wake region is resolved with the polynomial order $P = 7$ and the rest of domain has the order $P = 5$. The result is shown in Fig. 6. Comparing to the case of $P = 7$ the variable order leads to approximately 1.7 times better resolution close to the blade. The highest density equals $7.3 \cdot 10^7$ degrees of freedom per square unit in the trailing edge region. The total number of degrees of freedom increases from $\approx 3 \cdot 10^6$ at $P = 7$ to $\approx 3.5 \cdot 10^6$. We note also that the computational requirements with respect to CPU time are lower in the case of variable polynomial order.

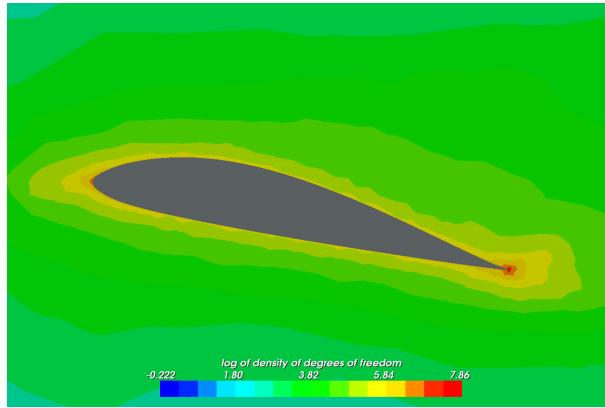


Figure 6: Density of degrees of freedom in the near airfoil region with variable polynomial order. The highest density at the trailing edge equals $7.3 \cdot 10^7$ degrees of freedom per square unit.

5 FIRST RESULTS

Currently the simulation is not quite advanced to collect statistical data. So, the presented results are based on the instantaneous data and describe the flow behaviour in a qualitative sense.

Considering the instantaneous pressure field (Fig. 7, right), high pressure gradients on the suction side of the blade close to the trailing edge are observed. Further it can be noted that there are several large vortex-like structures in the region $0.5 < x/cl < 1$ at the suction side of airfoil (Fig. 7, left and right).

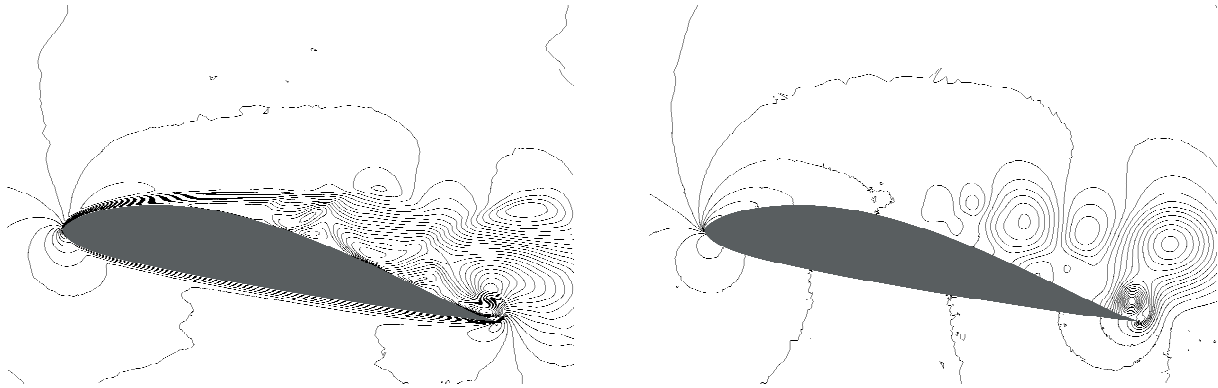


Figure 7: Contours of the instantaneous streamwise velocity (left) and the pressure (right).

Fig. 8 displays the instantaneous velocity fields in the interval $0.3 < x/cl < 0.5$ at the suction side (left) and around the trailing edge (right). One can see the flow separation at $x/cl = 0.3$ without a fully formed separation bubble. The right picture shows the separation region at the trailing edge.

In Fig. 9 the isosurfaces of instantaneous spanwise velocity are depicted. They can

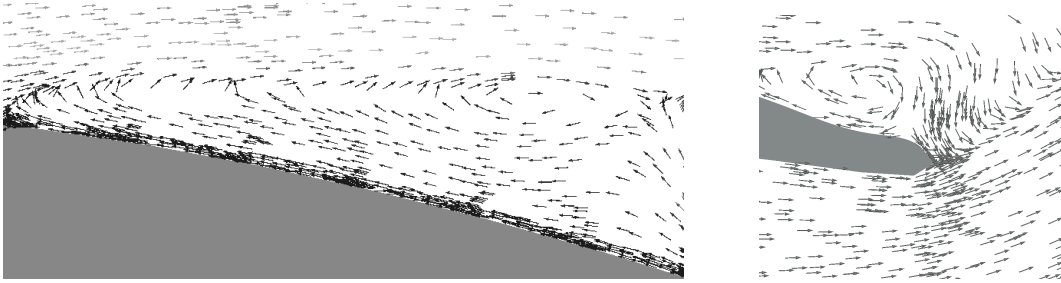


Figure 8: The instantaneous velocity field (scaling off) on the suction side of airfoil between $x/cl = 0.3$ and $x/cl = 0.5$ (left) and around the trailing edge (right).

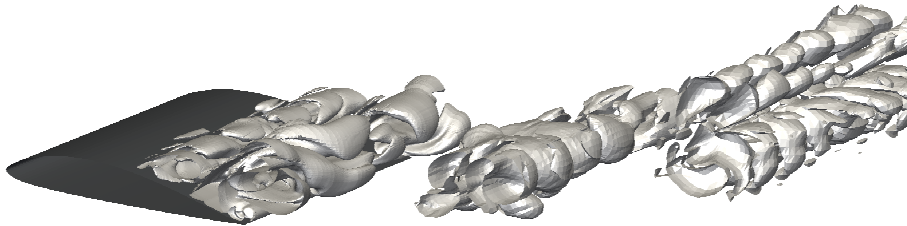


Figure 9: Instantaneous spanwise velocity (contour levels at $0.02U_\infty$).

be considered as a characteristic of the transition and growth of the turbulent boundary layer. The spanwise velocity reaches the value of $0.02U_\infty$ at $x/cl \approx 0.5$ and increases approaching the wake region.

6 CONCLUSIONS

In the paper we consider some aspects of LES of turbulent flow around the FX-79-W151 airfoil profile at Reynolds number $Re = 5 \cdot 10^3$ and angle of attack $\alpha = 12^\circ$ using high-order spectral/hp element method. So far most of the attention has been paid to the numerical method and the mesh generation problems. Due to the early stage of the currently performed simulation, we discuss some qualitative characteristics of the investigated flow.

The study of turbulent flow around a wind turbine blade, being a part of research project "Innovation und neue Energietechnologien" funded by the BMWA, Germany, will be continued. In the future we will perform also LES of turbulent flow for high Reynolds numbers, for higher angle of attack and using time variable inflow boundary conditions.

7 ACKNOWLEDGMENTS

We are grateful to Dr. S.Sherwin for the providing of the spectral/hp element code $\mathcal{N}\epsilon\kappa\mathcal{T}\alpha r$.

REFERENCES

- [1] L. Davidson, D. Cokljat, J. Fröhlich, M.A. Leschziner, C. Mellen and W. Rodi (eds.), *LESFOIL: Large Eddy Simulation of Flow Around a High Lift Airfoil*, Notes on Numerical Fluid Mechanics, Vol. 83, Springer Verlag, (2003).
- [2] N. Jovičić and Breuer M. High-Performance Computing in Turbulence Research: Separated Flow past an Airfoil at High Angle of Attack. *High Performance Computing in Science and Engineering*, 93-105,(2004)
- [3] M. Germano, U. Piomelli, P. Moin, W.H. Cabot. A dynamic subgrid scale eddy viscosity model, *Phys. of Fluids A*, vol. 3(7), 1760-1765, (1991)
- [4] S. Eisenbach and R. Friedrich. LES of the flow around an airfoil at $Re = 1 \cdot 10^5$ and high angle of attack using cartesian grids. *Large-Eddy Simulation of Complex Flows* EUROMECH Colloquium 469, TU Dresden, Germany, October 6-8, 2005
- [5] Th. Lerche, U. Ch. Dallmann. *Das Prinzipexperiment COSTWING I: Dokumentation der Aufbauphase*, Institut für Strömungsmechanik, DLR Göttingen, IB 223-99 A04, (1999).
- [6] Ch. Abegg. *Das Prinzipexperiment COSTWING II: Untersuchung kohärenter Strukturen in den Wanddruckschwankungen*, Institut für Strömungsmechanik, DLR Göttingen, IB 223-2001 A02, (2001).
- [7] K. Kindler, H.-P. Kreplin, D. Ronneberger. *Experimentelle Untersuchung kohärenter Strukturen in kritischen Tragflügelströmungen*, Interner Bericht, IB 224 - 2003 A 11, Inst. f. Aerodynamik und Strömungstechnik, DLR Göttingen, (2003).
- [8] H.-J. Kim, S. Lee, N. Fujisawa. Computation of unsteady flow and aerodynamics noise of NACA0018 airfoil using large eddy simulation. *Int. J. Heat and Fluid Flow*, **27**, 229-242, (2006)
- [9] X. Ma, G.-S. Karamanos, G.E. Karniadakis. Dynamics and low-dimensionality of a turbulent near wake. *J. Fluid Mech.*, **410**, 29-65, (2000)
- [10] G.E. Karniadakis and S. Sherwin. *Spectral/hp Element Method for CFD*. Oxford University Press, (1999)
- [11] T. Warburton. *Spectral/hp element methods on polymorphic domains*, PhD Thesis, Brown University (1998).

- [12] G.-S. Karamanos. *Large Eddy Simulation Using Unstructured Spectral/hp Elements*. PhD Thesis, Imperial Colledge, (1999)
- [13] G-S. Karamanos, S.J. Sherwin and J.F. Morrison. *Large-eddy simulation using unstructured spectral/hp elements*, in *Recent Advances in DNS and LES*, edited by D. Knight & L. Sakell, Kluwer Academic, Dordrecht/Norwell, MA, (1999).
- [14] A. Shishkin and C. Wagner. Direct Numerical Simulation of a turbulent flow Using a Spectral/hp element method, accepted for publication in Notes on *Numerical Fluid Mechanics*, Vieweg Publishers, Germany
- [15] B. Stoevesandt, A. Shishkin, J. Peinke and C. Wagner. Spectral/hp code simulation on airfoil for wind turbines, *ECCOMAS 2006, European Congress on Computational Methods in Applied Sciences and Engineering*, Ecmond an Zee, Nederlands, 2006.
- [16] G.E. Karniadakis, M. Israeli and S.A. Orszag. High-order splitting methods for incompressible Navier-Stokes equations, *J. of Comp. Phys.*, **97**, 414-443 (1991)